JOURNAL OF SOLID STATE CHEMISTRY 63, 237–249 (1986)

Phase Relation in the Oxygen Nonstoichiometric System, $SrFeO_x$ ($2.5 \leq x \leq 3.0$)

Y. TAKEDA, K. KANNO, T. TAKADA, AND O. YAMAMOTO

Department of Chemistry, Faculty of Engineering, Mie University, Tsu, Mie-ken, 514, Japan

AND M. TAKANO, N. NAKAYAMA, AND Y. BANDO

Institute for Chemical Research, Kyoto University, Uji, Kyoto-fu, 611, Japan

Received July 31, 1985

The $SrFeO_x$ system with $2.5 \leq x \leq 3.0$ was prepared and examined by differential thermal analysis, thermogravimetry, powder X-ray diffraction, and the ^{57}Fe Mössbauer effect. Four single phases with different structures exist in this system, the typical compositions of which are $SrFeO_3$, $SrFeO_{2.86}$, $SrFeO_{2.73}$, and $SrFeO_{2.50}$. $SrFeO_{2.86}$ and $SrFeO_{2.73}$ have newly found tetragonal and orthorhombic structures, respectively, and their unit cells are related to the cubic perovskite cell for $SrFeO_3$ in the manner that $a_t \approx 2 \times 2^{1/2} a_c$, $c_t \approx 2a_c$ and $a_o \approx 2c_o \approx 2 \times 2^{1/2} a_c$, $b_o \approx 2a_c$, where the suffixes c, t, and o stand for the cubic, tetragonal, and orthorhombic structures, respectively. These single-phase compositions suggest the ideal series of $SrFeO_{3-1/n}$, where $n = \infty$, 8, 4, and 2 give $x = 3$, 2.875, 2.75, and 2.50, correspondingly. The vacancy ordered phase of $SrFeO_{2.86}$, $SrFeO_{2.73}$, and $SrFeO_{2.50}$ show first-order transitions to their cubic, disordered structures at 250, 320, and 830°C, correspondingly. Formation of the cubic, disordered structure above a temperature depending on the composition is suggested for the whole composition range.

Introduction

The perovskite system of $SrFeO_x$ ($2.5 \leq x \leq 3$) is well known for containing Fe ions in the rare valence state of 4+ and also for the wide range of nonstoichiometry. $SrFeO_3$ containing only Fe^{4+} has the cubic perovskite structure, while $SrFe^{3+}O_{2.5}$ or $Sr_2Fe_2O_5$ crystallizes in an orthorhombic brownmillerite-like structure in which oxygen ions stringed along a particular direction of the parent perovskite structure are missing. However, various investigators have reported discrepant phase relations for the intermediate range of $2.5 < x < 3$. MacChesney *et al.* (*1*) were the first to undertake a systematic investigation on the preparation and characterization of this system and reported about 20 years ago that single phases with continuous oxygen content existed for $2.72 \leq x \leq 3$. The perovskite cell was cubic for $2.88 \leq x \leq 3$ and tetragonal for $2.72 \leq x \leq 2.84$. $SrFeO_{2.5}$ coexisted with a perovskite phase for $x = 2.60$. On the other hand, Tofield *et al.* (*2*) reported narrow single phase regions centered around the ideal compositions of $x = 3$, 2.75, and 2.5. The $x = 2.78$ phase near

0022-4596/86 $3.00

the ideal intermediate composition had an orthorhombic unit cell related to the perovskite cell by $a_o \approx 2 \times 2^{1/2} a_c$ and $b_o \approx 2a_c$ (suffixes o and c stand for the orthorhombic and cubic structures, respectively) as found by the electron diffraction (ED) method. However, this phase showed apparently cubic symmetry in its X-ray diffraction (XRD) pattern probably because of a microdomain structure.

As a part of our work on perovskite oxides containing highly charged Fe ions (*3*), we reported, in brief, the existence of the following phases found by measurements of XRD and the Mössbauer effect (ME) (*4*). These were the cubic perovskite phase for $2.9 \leq x \leq 3$, the tetragonal phase for $x \approx 2.85$ with $a_t \gtrsim c_t \approx a_c$ (suffix t indicating the tetragonal phase), the orthorhombic phase for $x \approx 2.75$ with $a_o \approx c_o \approx 2^{1/2} a_c$ and $b_o \approx a_c$, and $SrFeO_{2.5}$. Intermediate compositions between these were two phase mixtures. In that study, the ME proved to be very useful for the identification because each single phase exhibited its characteristic spectrum in both the paramagnetic and antiferromagnetic states. Then, Ea *et al.* (*5*) reported the cubic, tetragonal, and orthorhombic phases according to the compositions of $2.9 \leq x \leq 3$, $2.78 \leq x < 2.9$, and $x \approx 2.75$, and $SrFeO_{2.5}$. Finally, the composition-dependent ME spectra for $2.75 < x < 2.85$ were measured and interpreted as single-phase behavior by Gibb (*6*).

These discrepancies may be due to different methods of sample preparation and compositional analysis and also to difficulties in detecting slight structural distortions by XRD, the most widely applied method. The difficulties might arise not only from the instrumental limit but also be intrinsic from a tendency of microdomain formation as suggested by Tofield *et al.* (*2*) for the case of $x = 2.78$. Coherently packed microdomains of a single phase or mixed phases could give a monophasic diffraction pattern of seemingly high symmetry (*7*) leading to an erroneous phase identification. To obtain the conclusive phase relation, we have renewed our study by preparing more than 30 different samples under various conditions with respect to the oxygen partial pressure and temperature, analyzing them chemically and thermally, and by examining them with a powerful XR diffractometer, an electron microscope, and a ME spectrometer. As a result, we have confirmed our previous study, with modifications required from detection of very weak superlattice XRD peaks and corresponding ED spots indicative of enlarged unit cells for the tetragonal and orthorhombic phases, and found evidences of the first-order structural changes corresponding to order–disorder transitions of the oxygen vacancies in $SrFeO_{2.86}$, $SrFeO_{2.73}$, and $SrFeO_{2.50}$. Formation of the disordered cubic perovskite structure above composition-dependent temperatures is suggested for the whole composition range.

Sample Preparation

Samples were prepared as follows. $SrCO_3$ and α-Fe_2O_3, both being purchased from Nakarai Chemicals Ltd. and having a purity of 99.99%, were mixed in a molar ratio of 2 : 1 and, then, heated in the air at 1000°C for 24 hr. The products were ground, pressed into disks, and heated again in the air at 1300°C for 12 hr. Subsequent annealing was carried out at various temperatures between 250 and 1400°C in a stream of nitrogen (99.99% pure) of 1 atm, the air, or under oxygen pressures of 1–500 atm. The duration of annealing ranged from 24 to 300 hr depending on the temperature. To prevent rapid oxidation at lower temperatures, the samples annealed in N_2, the air, or O_2 of 1 atm were quenched in liquid N_2. Those treated under higher oxygen pressures were cooled rapidly by immersing the stellite autoclave in water. By this way we

could prepare samples covering a composition range of $2.50 \leq x \leq 2.97$.

The oxygen content was determined by two independent methods, chemical analysis and thermogravimetry. The chemical analysis was carried out with the method applied by Mori (*8*) to the $BaFeO_x$ system. This method takes advantage of the oxidation of Fe^{2+} ions in a standard solution to Fe^{3+} by highly charged Fe ions coming from a sample. The weight loss on heating sample powders to 1350°C in an N_2 stream of 1 atm to reduce to $SrFeO_{2.50}$ was measured by an automatic differential thermal analysis–thermogravimetry (DTA-TG) apparatus of Rigaku DTA-6 TG-4. These two kinds of measurements were in good agreement with each other so that $|x_{\text{chem.anal.}} - x_{\text{TG}}| \leq 0.03$. The compositions given below take values averaged over these two independent measurements.

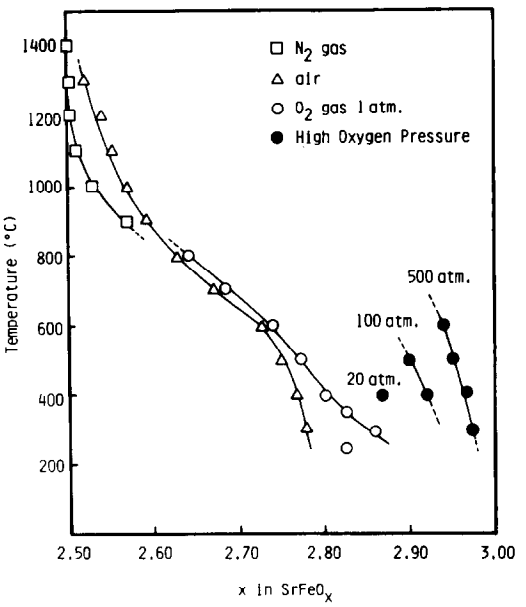

FIG. 1. Annealing temperature dependence of composition under various oxygen pressures.

Experimental Results and Discussion

1. Phases Present in the Quenched Samples

The relation between the equilibrating condition and the resulting oxygen content is plotted in Fig. 1. It is evident that annealing under a higher oxygen partial pressure at a lower temperature increases x. However, the oxygen diffusion within a crystal was slow at 250°C, making it difficult to attain equilibrium even after 300 hr.

XR diffractograms were obtained with both monochromated Cu$K\alpha$ and Cu$K\beta$ radiation by using equipment of Rigaku RU-200. A slight distortion from the cubic perovskite structure makes additional very weak reflections appear and splits most of the main reflections; such weak reflections were observed more distinctly with the intenser $K\alpha$ radiation, while slight splittings of the main reflections were observed with the singlet $K\beta$ radiation. Some typical diffraction peaks are compared in Fig. 2. Among all the samples except for $SrFeO_{2.50}$ with well-known structure, $SrFeO_{2.97}$, $SrFeO_{2.86}$, and $SrFeO_{2.73}$ exhibited the most well-defined diffractograms consisting of very sharp peaks with reasonable relative intensities. $SrFeO_{2.97}$ crystallizes in a simple cubic perovskite cell of $a_c = 3.855$ Å, $SrFeO_{2.86}$ in a tetragonal unit cell with $a_t = 10.937$ Å ($\approx 2 \times 2^{1/2} a_c$) and $c_t = 7.705$ Å ($\approx 2a_c$), and $SrFeO_{2.73}$ in an orthorhombic cell with $a_o = 10.972$ Å ($\approx 2 \times 2^{1/2} a_c$), $b_o = 7.700$ Å ($\approx 2a_c$), and $c_o = 5.471$ Å ($\approx 2^{1/2} a_c$). The observed and calculated data are compared in Table I.

In comparison with these phases, the other compositions like $x = 2.94$, 2.80, and 2.68 have slightly broadened main peaks and vague superlattice peaks. The main peaks shift to slightly lower angles according to a tendency that the volume per molecule increases with decreasing x as if these are single-phase materials with continuous oxygen content. However, as will be described later, the ME study eliminated this possibility except for the case of $SrFeO_{2.68}$.

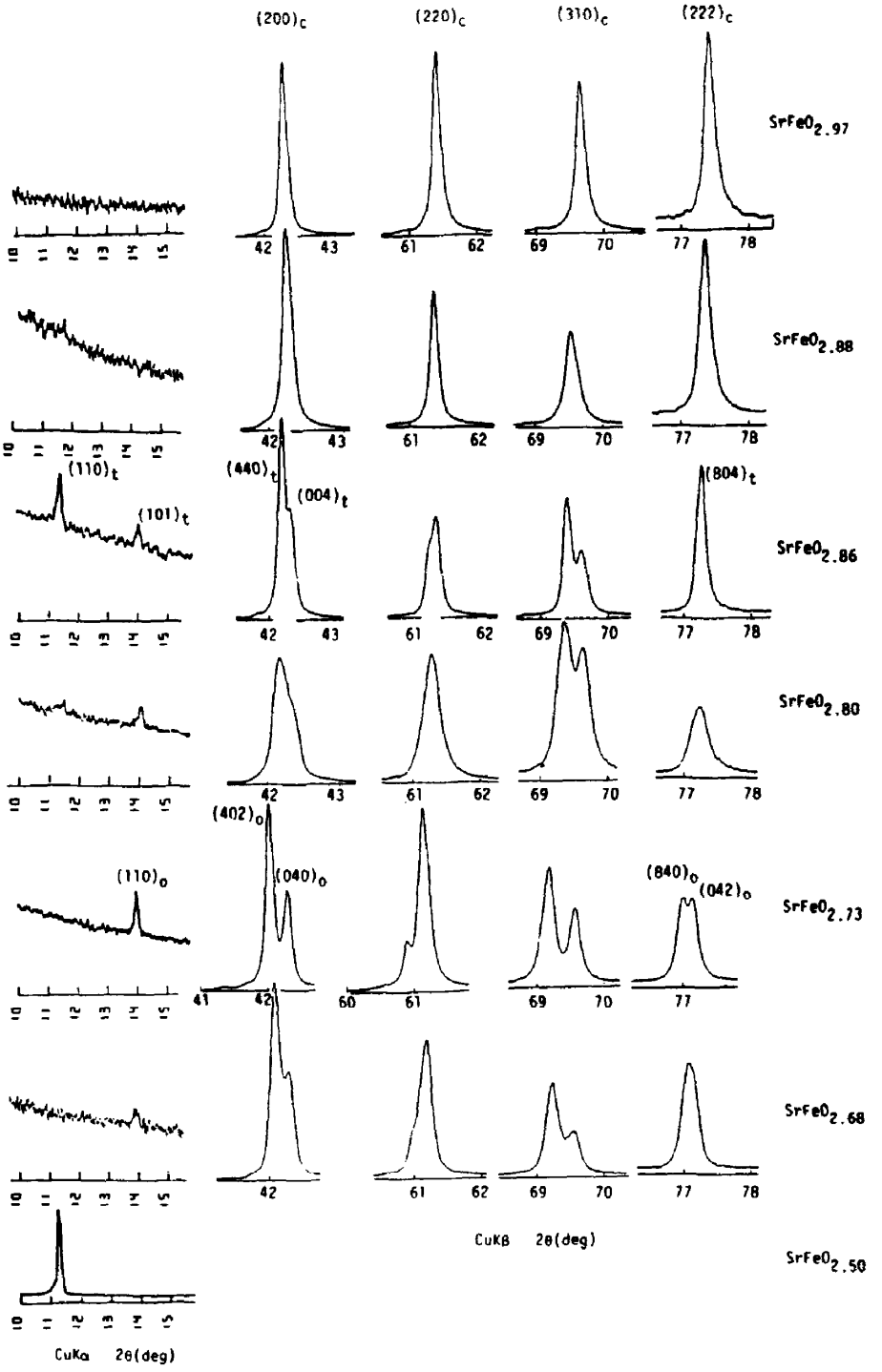

FIG. 2. XRD line profiles of $SrFeO_x$. The peak heights are adjusted to facilitate comparison of the lineshape.

TABLE I

X-RAY DATA FOR $SrFeO_{2.97}$, $SrFeO_{2.86}$, AND $SrFeO_{2.73}$

	$SrFeO_{2.97}$ a = 3.855(3) Å			$SrFeO_{2.86}$ a = 10.934(6) Å c = 7.705(5) Å				$SrFeO_{2.73}$ a = 10.972(6) Å b = 7.700(5) Å c = 5.471(3) Å			
hkl	d_{obs}	d_{cal}	*I*	*hkl*	d_{obs}	d_{cal}	*I*	*hkl*	d_{obs}	d_{cal}	*I*
				110	7.75	7.73	≪1				
				101	6.28	6.30	≪1	110	6.31	6.30	1
				200	5.43	5.47	≪1	200 001	5.46	5.49 5.47	≪1
								111	4.14	4.13	<1
100	3.858	3.855	3	211	3.867	3.866	2	201	3.871	3.871	3
				112	3.453	3.448	≪1				
110	2.727	2.726	100	400 222	2.732	2.734 2.729	100	400 002 221	2.734	2.743 2.736 2.731	100
				141 103	2.505	2.508 2.500	<1	112 130	2.509	2.509 2.502	1
111	2.224	2.226	20	402	2.229	2.229	15	420 022	2.231	2.234 2.230	11
				332	2.145	2.142	<1				
				510 341	2.103	2.104 2.104	<1	510	2.110	2.110	1
200	1.927	1.928	80	440	1.936	1.933	25	402	1.937	1.937	30
				004	1.928	1.926	12	040	1.926	1.925	15
				530	1.874	1.875	≪1				
210	1.725	1.724	<1	620 442	1.728	1.729 1.728	<1	601	1.734	1.734	1
								203 422	1.731	1.731 1.730	1
				224	1.724	1.724	1	241	1.724	1.724	1
								512	1.671	1.671	<1
211	1.574	1.574	30	622 404	1.577	1.577 1.575	14	621 223 440 042	1.578	1.581 1.578 1.576 1.574	20
								710	1.536	1.536	≪1
								532	1.426	1.431	≪1
220	1.363	1.363	25	800	1.366	1.367	8	800	1.372	1.372	3
				444	1.365	1.364	8	004 442	1.366	1.368 1.365	12
								152	1.333	1.332	≪1
221	1.285	1.285	<1	624	1.287	1.287	1	641 243	1.288	1.289 1.287	1
								552	1.261	1.261	≪1
310	1.219	1.219	15	840 662	1.222	1.222 1.222	7	802 404 623	1.225	1.226 1.224 1.224	9
				226	1.219	1.219	4	261	1.219	1.218	9
								732	1.202	1.202	≪1
311	1.162	1.162	5	842	1.165	1.165	2	822	1.168	1.168	1
222	1.113	1.113	8	804	1.114	1.115	5	840	1.117	1.117	3
								042	1.115	1.115	3
320	1.069	1.069	<1								
321	1.030	1.030	10	1022	1.033	1.033	7	1021	1.036	1.036	4
				844 626	1.031	1.032 1.031	4	225 842 442	1.034	1.034 1.034 1.033	6

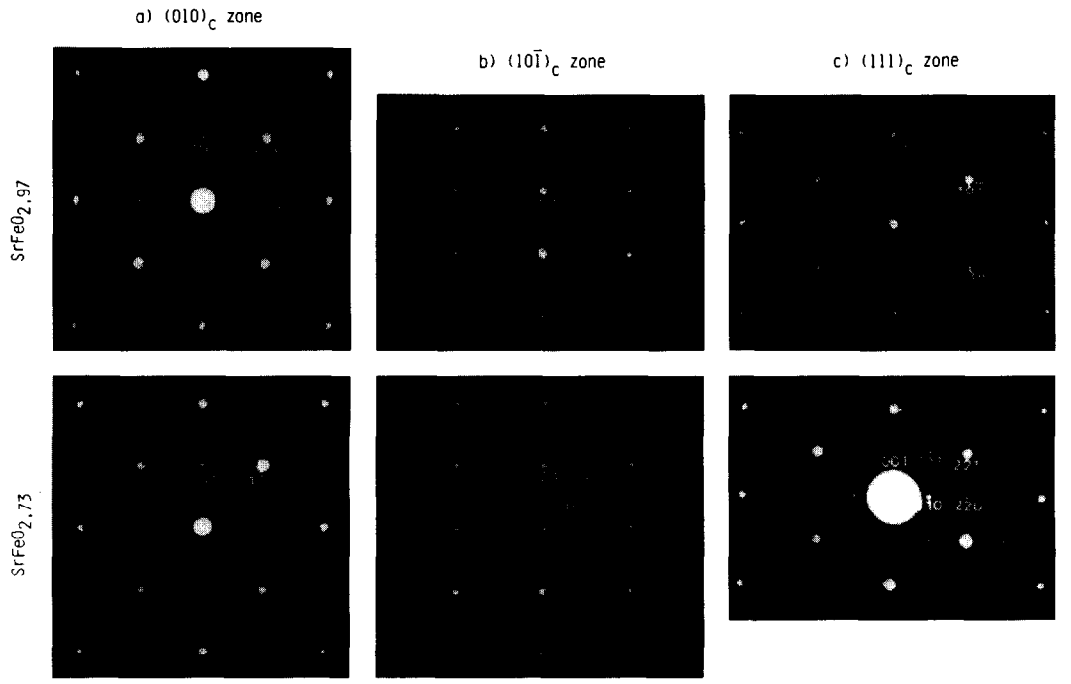

FIG. 3. Electron diffraction patterns of cubic $SrFeO_{2.97}$ and orthorhombic $SrFeO_{2.73}$. Zone axes are (a) $(010)_c$, (b) $(101)_c$, and (c) $(111)_c$.

Electron diffraction measurements made with an apparatus of JEM 100CX on $SrFeO_{2.97}$, $SrFeO_{2.86}$, and $SrFeO_{2.73}$ gave microscopic evidence supporting our XRD analysis. The representative ED patterns of $SrFeO_{2.97}$ and $SrFeO_{2.73}$ are shown in Fig. 3. Those of $SrFeO_{2.97}$ consist merely of the cubic perovskite-type basic spots, while some additional superspots appear in the patterns for $SrFeO_{2.73}$. The $2 \times 2^{1/2}\, a_c * 2a_c * 2^{1/2}a_c$ supercell and the extinction conditions for $SrFeO_{2.73}$ are completely consistent with the XRD measurements. $SrFeO_{2.86}$ also showed such superspots that indicate a supercell of $2 \times 2^{1/2}a_c * 2 \times 2^{1/2}a_c * 2a_c$ which agrees, in principle, with the XRD results. However, possible changes in the structure and oxygen content caused by electron beam irradiation made a detailed analysis difficult. These problems were much less serious for $SrFeO_{2.73}$.

The ME spectra obtained at 295 and 4 K are shown in Fig. 4. It is very clear that, in either of the paramagnetic and antiferromagnetic states, $SrFeO_{2.97}$, $SrFeO_{2.86}$, $SrFeO_{2.73}$, and $SrFeO_{2.68}$ show their characteristic spectra, while the other compositions show mixed ones. For example, the $SrFeO_{2.97}$- and $SrFeO_{2.86}$-types show mixed spectra for $x = 2.94$, and those for $x = 2.80$ reveal the coexistence of $SrFeO_{2.86}$ and $SrFeO_{2.73}$. $SrFeO_{2.68}$ was detected clearly for $x = 2.51$. Spectra from many other compositions also could be explained by mixing the ones for the relevant couples of single phases with composition dependent ratios. Of particular interest is the composition of $x = 2.88$. Though the XRD pattern is almost of the cubic perovskite type as can be seen in Fig. 2, the ME spectra are close to those of the tetragonal phase. The following situation is highly possible. A crystallite of $x =$

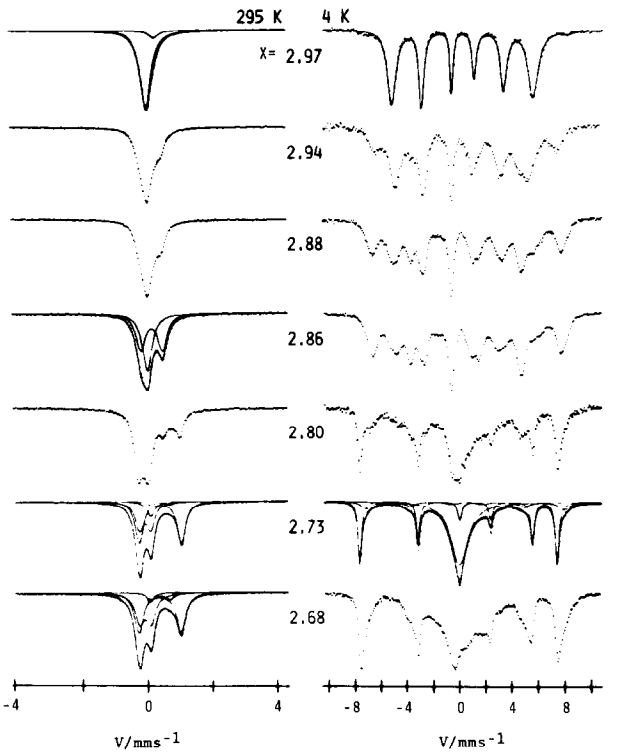

FIG. 4. Mössbauer spectra of $SrFeO_x$ at 295 and 4 K. The solid lines are the computed fits (see Table II).

2.88 consists of two kinds of microdomains having structures and compositions appropriate to the cubic ($x \approx 3$) and tetragonal ($x \approx 2.86$) phases, the majority being of the latter type. The domains are coherently packed, the c axis of the tetragonal phase changing randomly from one of the sixfold equivalent directions corresponding to $\langle 100 \rangle_c$ to another from domain to domain. So, it is an averaged, seemingly cubic structure that was observed by XRD. For $x = 2.94$, the number and total volume of the cubic microdomains would be increased to make the averaged unit cell volume smaller as experimentally observed. A similar situation would hold also in the intermediate region between the tetragonal and orthorhombic phases where almost monophasic XRD properties were observed. Anyway, the most important conclusion to be drawn here is that the single phases present in the quenched samples have rather narrow composition ranges of $2.97 \lesssim x \leq 3$, $x \approx 2.86$, $2.68 \lesssim x \lesssim 2.73$, and $x \approx 2.50$.

The ME spectra obtained from the single phases were analyzed by computer fitting assuming the Lorentzian lineshape. The results are, as a matter of course, very similar to those reported in our previous paper (*4*). As a new important result, we assign the quadrupole doublet for $SrFeO_{2.86}$ to an unusual state between Fe^{3+} and Fe^{4+}, that is $Fe^{3.5+}$. The parameter values, assignment, and the oxygen contents estimated by this method are summarized in Table II. We should stress here that the distribution of the d electrons on highly charged Fe ions

TABLE II

MÖSSBAUER DATA OF $SrFeO_x$

Sample x	300 K					4 K				
	IS, mm sec^{-1}	ΔE, mm sec^{-1}	%	Valence	X_M[a]	IS, mm sec^{-1}	ΔE, mm sec^{-1}	Hi/T	Valence	%
2.97	0.06	—	94	Fe^{4+}	2.97	0.2	—	33	Fe^{4+}	95
	0.32	—	6	Fe^{3+}		0.4	—	51	Fe^{3+}	5
2.86	0.04	—	45	Fe^{4+}	2.86	0.0	—	~29	$Fe^{(4+\delta)+}$	50
	0.17	0.84	55	$Fe^{3.5+}$		0.4	—	~44	$Fe^{(4-\delta)+}$	30
2.73	−0.09	0.34	33	Fe^{4+}	2.71	Very broad absorption centered around ~0 mm sec^{-1}				48
	0.11	—	9	Fe^{4+}						
	0.37	1.29	53	Fe^{3+}		0.5	−1.29	46	Fe^{3+}	38
	0.35	0.58	5	Fe^{3+}		0.4	0.3	47	Fe^{3+}	14
2.68	−0.11	0.35	33	Fe^{4+}	2.71	Very broad absorption centered around ~0 mm sec^{-1}				47
	0.09	—	8	Fe^{4+}						
	0.36	1.27	51	Fe^{3+}		0.5	−1.29	46	Fe^{3+}	24
	0.37	0.56	8	Fe^{3+}		0.4	0.3	47	Fe^{3+}	29

[a] X_M represents the oxygen contents estimated by the assignments shown in this table.

is very versatile, changing not only with the ratio and kind of the alkaline earth and rare earth cations and temperature as observed in the stoichiometric systems of $Ca_{1-u}Sr_uFeO_3$ and $Sr_{1-v}La_vFeO_3$ etc. (*3*) but also with the oxygen content as revealed in the present nonstoichiometric system; the isomer shift and magnetic hyperfine field, both being related to the *d* electron number, take a wide range of values (see Table II). These data are useful for putting restrictions on possible structural models deduced from the diffraction properties, since the electronic state of the Fe ion examined by the ME seems to be sensitive to the surroundings and, therefore, reflects the vacancy-ordering scheme. A further discussion on the ME data and compatible structural models will be reported elsewhere.

The ME spectra for $2.75 < x < 2.85$ obtained and interpreted as monophasic by Gibb (*6*) can be explained more consistently by considering phase mixing as shown below. Firstly, the composition dependence of the spectrum at room temperature shows the same tendency as observed and interpreted as mixed phase behavior in the present paper. For example, the peak at ≈1 mm/sec of the component named "X" in Ref. (*6*) which becomes more intense with decreasing oxygen content is a characteristic peak of $SrFeO_{2.73}$, and the peak at ≈0.5 mm/sec from component "Y" belongs to $SrFeO_{2.86}$. Second, the change of component X from a quadrupole doublet to a magnetic hyperfine pattern below 220 K and the similar change of component Y at a much lower temperature of ≈85 K are certain evidence of the coexistence of the tetragonal and orthorhombic phases having different Nèel temperatures (T_N); according to Refs. (*1*, *5*), $T_N \approx 235$ K for $x = 2.75$, and $T_N \approx 80$ K for $x = 2.84$. Third, the single-peak spectrum due to a thermally excited electron exchange for $x = 2.844$ at 700 K (the oxygen content decreased during the measurement under vacuum!) interpreted as being strong evidence of monophasic behavior should have been examined more carefully. As described later, $SrFeO_{2.86}$ and $SrFeO_{2.73}$ show transitions to their cubic, vacancy-disordered structures at different temperatures below 700 K. Our preliminary ME measurements at elevated temperatures on samples sealed in silica tubes have revealed that each phase shows its own characteris-

tic behavior including appearance of a single peak at its characteristic temperature.

The ME spectrum at room temperature and the ED patterns of $SrFeO_{2.78}$ measured by Tofield *et al.* (*2*) are considerably different from those obtained in the present study. Their spectrum has a character intermediate between those for $SrFeO_{2.86}$ and $SrFeO_{2.73}$ suggesting a composition of $x > 2.73$, and the unit cell deduced from their ED patterns is doubled along the c-axis ($c_o \approx 2 \times 2^{1/2} a_c$) in comparison with the present one ($c_o \approx 2^{1/2} a_c$), as it is for $SrFeO_{2.86}$. Thus, it seems possible that their sample was a mixture of the tetragonal and orthorhombic phases.

2. Thermodynamical Behavior at Elevated Temperatures

The above-mentioned examinations on the samples quenched from various temperatures and oxygen partial pressures had only limited significance in the elucidation of the phase relations. So, the thermodynamical behavior was investigated by DTA, TG, and XRD. Samples were kept in a stream of nitrogen (99.99% pure) of 1 atm in a temperature range between 20 and 1350°C. The representative DTA-TG curves measured at a rate of 10°C/min are shown in Fig. 5. It is evident that each single phase of $x = 2.50$ 2.68, 2.73, and 2.86 has an endothermic DTA peak on heating, exothermic on cooling, which is not accompanied by a gravimetric change. The peaks for $x = 2.50$, 2.68, and 2.73 correspond definitely to their crystalline transitions to cubic perovskite symmetry as revealed by XRD. $SrFeO_{2.86}$ also seems to show the same kind of transition as will be discussed later. The transition temperature determined from the crossing point of the baseline and the steepest slope on the low-temperature side of the peak on heating and on the high-temperature side on cooling is 830, 320, 325, and 250°C for $SrFeO_{2.50}$, $SrFeO_{2.68}$, $SrFeO_{2.73}$, and $SrFeO_{2.86}$, correspondingly. Hysteresis was small, at most 10°C, not much above experimental error.

The temperature dependence of the lattice constants and the volume per molecule of $SrFeO_{2.50}$ are shown in Fig. 6. The constants tend to become longer with increasing temperature and coalesce into the unique one for the cubic phase at higher temperatures. The transition seems to be of first order since it is accompanied by a discontinuous change in volume extrapolated to 830°C and a latent heat. Most probably, the oxygen vacancies are disordered in the cubic phase. Incidentally, these results are considerably different from those reported by the previous investigators. According to Shin *et al.* (*9*), the transition temperature was 700°C and the unit cell volume changed without a jump. Ea *et al.* (*5*) found two DTA peaks at 350 and 850°C[1] and their XRD measurements indicated the coexistence of two types of structures in the temperature range of $350 < T < 850$°C, one the normal brownmillerite structure and the other a tetragonal perovskite structure. According to our DTA measurements on various compositions, double peaks appear and, at the same time, the second peak is shifted to below 830°C only when $SrFeO_{2.68}$ coexists. For example, they were detected at 310 and 730°C for $x = 2.53$ and at 310 and 640°C for $x = 2.57$. The samples studied by the previous investigators seem to have been of $x > 2.50$. These observations suggested, on the other hand, that the compositions of $2.50 < x < 2.73$ become single cubic perovskite phases having continuous oxygen content above the temperatures of

[1] The transition temperatures of 350 and 850°C were determined from the positions of the DTA peaks. By applying the more reasonable way of using the crossing point of the baseline and the steepest slope on either side of the peak taken in the present study, these should be read as 320 and 770°C.

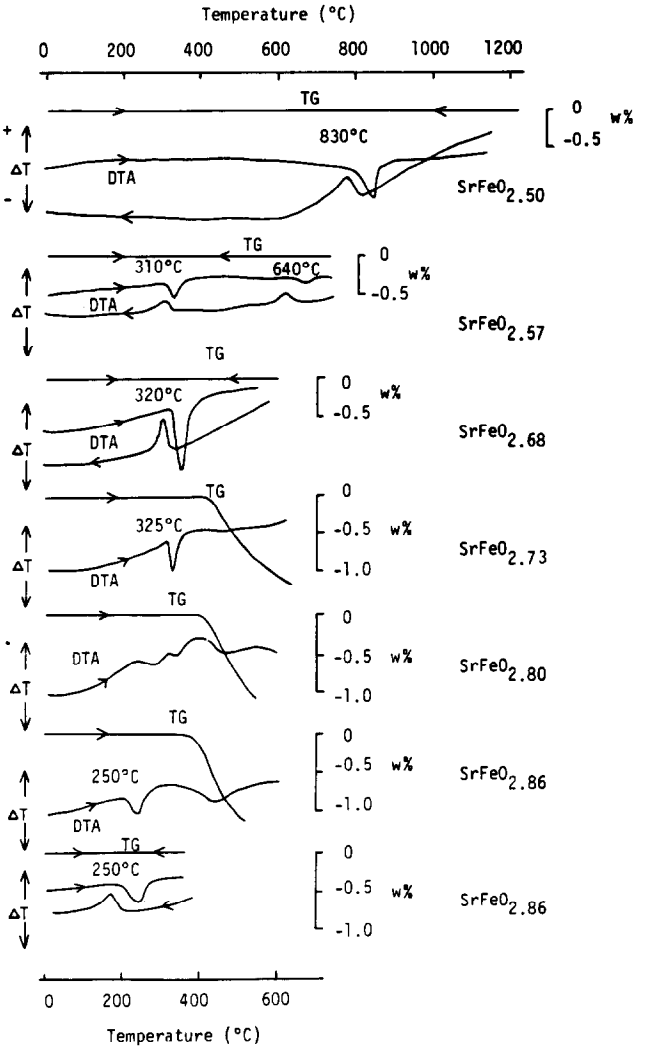

FIG. 5. DTA-TG curves of $SrFeO_x$ measured at a rate of 10°C/min in a stream of nitrogen (99.99% pure) of 1 atm.

the second DTA anomaly, which is plotted against x in Fig. 7. The first DTA anomaly indicates the transition of the coexistent perovskite phase, $SrFeO_{2.68}$, to its cubic structure. With increasing temperature, the amount of the brownmillerite phase decreases and a grossly oxygen-deficient perovskite phase of $x < 2.68$ is formed. The second DTA anomaly corresponds to the uniform formation of the cubic perovskite. Therefore, the second anomaly must be absent when temperature is raised slowly enough to attain the equilibrium state. XRD peak profiles consistent with the above interpretation were obtained for $x = 2.56$ at various temperatures below 700°C both on heating and cooling.

XRD peak profiles of $SrFeO_{2.73}$ obtained

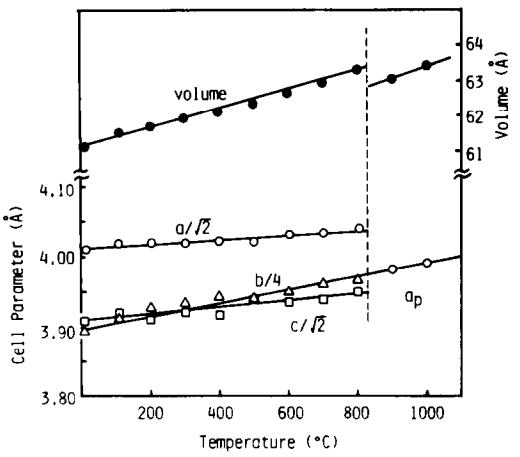

FIG. 6. Temperature dependence of the lattice constants and the volume per molecule of $SrFeO_{2.50}$. The orthorhombic lattice constants are reduced to $a/\sqrt{2}$, $b/4$, and $c/\sqrt{2}$ for comparison with the cubic lattice constant (a_p) of the high-temperature phase.

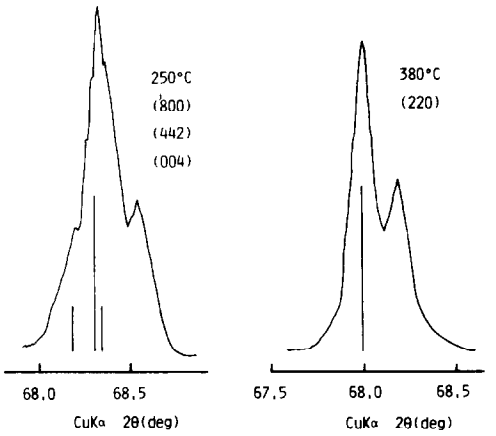

FIG. 8. XRD line profiles of $SrFeO_{2.73}$ at 250 and 380°C.

below and above the transition temperature are compared in Fig. 8. A cubic pattern was obtained at 380°C. On the other hand, Sr $FeO_{2.86}$ tended to lose its oxygen during XRD measurements, making exact identification of the high-temperature phase difficult. However, it is quite natural to assume its cubic phase, the transition taking place at a lower temperature than that for Sr $FeO_{2.73}$ because of the lower vacancy concentration. An intermediate composition of $x = 2.80$ exhibited double DTA peaks reflecting the coexistence of the tetragonal and orthorhombic phases transforming at different temperatures. Considering that the cubic structure is stabilized at room temperature for $x \geq 2.97$, we assume that the cubic, disordered structure is formed above composition-dependent temperatures for the whole composition range.

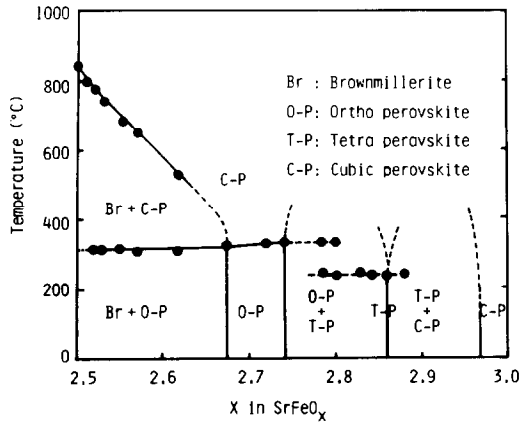

FIG. 7. Pseudobinary phase diagram representing the phase relation as a function of the oxygen content and temperature. Black circles indicate the transition temperatures determined by DTA.

Very recently, Mizusaki *et al.* (*10*) made an *in situ* measurement of the oxygen content through the change in the sample weight as a function of oxygen partial pressure and temperature within a range of 10^{-5} (atm) $\leq pO_2 \leq 1$ and 500°C $\leq T \leq$ 900. Their results indicated three kinds of pO_2-T regions where the brownmillerite phase and a perovskite phase exist singly and together, which is consistent with our study.

Finally, we comment on the stability of microdomain structure examined by annealing for 30 days at 230°C powders of Sr $FeO_{2.82}$ sealed in a Pylex glass tube to maintain the oxygen content. In this

composition, almost equal amounts of the tetragonal and orthorhombic phases are expected to coexist by forming a microdomain structure. It was expected that the prolonged annealing below the structural transition temperature of the tetragonal phase might increase its domain size to change the original monophasic XRD pattern to such a one manifesting the coexistence of the two phases. The annealing temperature was expected to be not too low to activate rearrangement of the oxygen vacancies as it is near the vacancy-disordering temperature of the tetragonal phase. However, as a result, no meaningful change was detected. The present result and the thermoanalytical study revealing the reversible structural transitions indicate that the microdomain structure is not a metastable state created by the rapid quenching from a higher temperature but the thermodynamically stable state.

Summary

The results of the present study can be outlined as follows. $SrFeO_x$ ($2.5 \leq x \leq 3$) forms the cubic, vacancy-disordered perovskite structure above composition-dependent temperatures. On cooling, the system is finally disproportionated into Sr $FeO_{2.50}$, $SrFeO_{2.68-2.73}$, $SrFeO_{2.86}$, and $SrFeO_{2.97-3}$. The structures and electronic states have been studied with the methods of XRD, ED, and ME. The oxygen vacancies in the three preceding phases create order–disorder transitions at 830, 320, and 250°C, while the phase of the compositions of $x \geq 2.97$ keeps its disordered structure to room temperature. The compositions of these ordered phases lead us to assume a series of the ideal compositions of Sr $FeO_{3-1/n}$, where $n = \infty$, 8, 4, and 2 give $x =$ 3, 2.875, 2.75, and 2.5, correspondingly. A further discussion on the ME data reflecting the vacancy-ordering scheme and compatible structural models will be reported elsewhere. Referring to the intermediate compositions, the facts that the rapid quenching from the final annealing temperatures could not prevent the phase separation as revealed by the ME in spite of the almost monophasic XRD properties, the quick single cubic phase formation on heating observed by measurements of DTA and XRD on various compositions, and the absence of the annealing effect suggest that couples of neighboring phases tend to coexist by forming coherently packed stable microdomains and, therefore, the formation and separation of the single phases led by oxygen diffusion through the boundaries are facilitated.

It seems interesting to study the high-temperature cubic phase from the viewpoint of structure and chemical properties. Disordering of the vacancies would proceed via a short-range ordered state. In fact, our preliminary ME measurements on $SrFeO_{2.50}$ suggested persistence of a short-range ordered state in the similarity of the spectra obtained below and above the transition temperature. The microdomain model for the cubic phase of $SrFeO_{2.50}$ proposed by Grenier *et al.* (*5*) may correspond to such a short-range ordered state that would not induce a serious change in the ME spectrum. According to Shin *et al.* (*11*), nitrogen monoxide, NO, is catalytically decomposed into nitrogen and oxygen by cubic $SrFeO_{2.5}$, and unidentified oxygen-rich perovskite phases absorb NO into their cystalline lattices at temperatures of 200 ~ 400°C. It is, we believe, highly possible that the transition to the disordered structure enhances a chemical activity of $SrFeO_x$ to NO. Investigations on these problems are now in progress.

Acknowledgments

We thank Professors K. Kamiya and T. Yoko at Mie University for the use of high temperature X-ray dif-

fractometer. The expense of this study was defrayed by a Grant in Aid for Special Research Project from the Ministry of Education.

References

1. J. B. MacChesney, R. C. Sherwood, and J. F. Potter, *J. Chem. Phys.* **43,** 1907 (1965); P. K. Gallagher, J. B. MacChesney, and D. N. E. Buchanan, *J. Chem. Phys.* **41,** 2429 (1964).
2. B. C. Tofield, C. Greaves, and B. E. F. Fender, *Mater. Res. Bull.* **10,** 737 (1975); B. C. Tofield, *React. Solids [Proc. Int. Symp.] 8th,* 253 (1976).
3. M. Takano and Y. Takeda, *Bull. Inst. Chem. Res. Kyoto Univ.* **61,** 406 (1983), and references therein.
4. M. Takano, N. Nakanishi, Y. Takeda, and T. Shinjo, *in* "Ferrites, Proc. Int. Conf., 1980, Japan" (H. Watanabe, S. Iida, and M. Sugimoto, Eds.), p. 389, Center for Academic Publication, Japan (1981).
5. N. Ea, These Docteur 3em cycle, Universite de Bordeaux 1 (1983); J.-C. Grenier, N. Ea, M. Pouchard, and P. Hagenmuller, *J. Solid State Chem.* **58,** 243 (1985).
6. T. C. Gibb, *J. Chem. Soc. Dalton Trans.*, 1455 (1985).
7. J. S. Anderson, *in* "Problems of Nonstoichiometry" (A. Rabenau, Ed.), Chap. 1, North-Holland, Amsterdam/London (1970).
8. S. Mori, H. Hirata, and N. Tonoka, *Japan Anal.* **16,** 1340 (1967).
9. S. Shin, M. Yonemura, and H. Ikawa, *Mater. Res. Bull.* **13,** 1017 (1978).
10. J. Mizusaki, private communication.
11. S. Shin, Y. Hatakeyama, K. Ogawa, and K. Shimomura, *Mater. Res. Bull.* **14,** 133 (1979).